

Hydrolytic Aging of Polycarbonate. I. Physical Aspects

I. GHORBEL,^{1,*} F. THOMINETTE,² P. SPITERI,³ and J. VERDU^{2,†}

¹ENSMP, B.P. 3, 91000 Evry Cedex, France, ²ENSAM, 151 Boulevard de l'Hôpital, 75013 Paris, France, and ³EDF, Centre de Recherche des Renardières, B.P. 1, 77250 Moret/Loing, France

SYNOPSIS

The hydrolytic aging of an unstabilized industrial sample of polycarbonate was studied at 40, 70, 80, and 90°C, 100% RH. The water absorption characteristics show that, at equilibrium, the polymer absorbs about 0.04 mol water per ester group and that the equilibrium is reached after about 10–40 h exposure, i.e., far before irreversible changes of physical properties are observed. Differential scanning calorimetry reveals the combined effects of hydrolytic chain scission and physical aging on glass transition temperature. Investigations on tensile yield properties showed that hydrolytic chain scission leads to a significant decrease of the apparent Eyring's activation volume. These observations strongly support the hypothesis that there are preexisting or hydrolysis-induced defects responsible for an heterogeneous distribution of chain scissions that would be concentrated into localized microdomains. © 1995 John Wiley & Sons, Inc.

INTRODUCTION

When exposed to wet conditions at moderate temperature below its glass transition temperature (150°C), the bisphenol A polycarbonate (PC) undergoes physical and chemical aging, this latter being due to random chain scission resulting of the carbonate ester hydrolysis.^{1–7} From a practical viewpoint, the most important consequence of this process is that the initially ductile polymer becomes brittle when its molar mass M_n becomes lower than a critical value M_{nc} , for instance, $M_{nc} = 14 \text{ kg mol}^{-1}$ according to Gardner and Martin.⁸

This behavior could be described in terms of structural changes at the macromolecular level. In this case, M_{nc} would correspond to the entanglement limit M_c below which plastic deformation cannot occur so that brittle rupture takes place. We believe, however, that the embrittlement mechanism is not so simple. These reasons could be summarized as follows:

1. Physical aging is linked to the nonequilibrium character of the glassy state and superimposes its effects to that of hydrolytic degradation. It is well known that physical aging can be also responsible for embrittlement.⁹
2. There is no experimental proof that $M_{nc} = M_c$. In other words, the aging-induced ductile-brittle transition does not necessarily occur at the same molar mass value as for undegraded samples. Elastic measurements in rubbery state or rheometric measurements in molten state seem to give considerably lower values than the one cited above: $M_c \approx 3 \text{ kg mol}^{-1}$.¹⁰ Some doubt subsists, however, on the consistency of molecular mass determination methods used in these studies so that it is difficult to reach definitive conclusions on this field.
3. There are reasons to suppose that, despite the relatively high initial homogeneity of the glassy polycarbonate, hydrolysis can be, in its early period or after a critical conversion, concentrated in microdomains capable of playing a role in the initiation of brittle rupture. As a matter of fact, the growth of osmotic disk-shaped cracks has been observed,¹¹ the propagation mechanism is now well un-

* Present address: ENS de Cachan, LMT, 61 Av. du Pdt Wilson, 94235 Cachan Cedex.

† To whom correspondence should be addressed.

Journal of Applied Polymer Science, Vol. 55, 163–171 (1995)

© 1995 John Wiley & Sons, Inc.

CCC 0021-8995/95/010163-09

derstood, whereas the initiation mechanism remains unknown.

The aim of this article is to investigate the physical aspects of polycarbonate hydrolysis in glassy state in order to try to bring about new data to help elucidate the embrittlement mechanisms. Particular attention has been paid to the degradation effects on the mechanical yielding kinetic regime, in order to put in evidence an eventual change of the Eyring's activation volume.

EXPERIMENTAL

Material

The polymer was an industrial-grade of LEXAN polycarbonate (General Electric Plastics). Its number-average molar weight determined by steric exclusion chromatography (SEC) with a polystyrene calibration was $M_n = 46 \text{ kg mol}^{-1}$. Its density was $\rho = 1.20 \text{ g/cm}^3$ and its glass transition temperature determined by differential scanning calorimetry (DSC) was $T_g = 154^\circ\text{C}$. Its mechanical spectrum (METRAVIB, 5 Hz, 5 K min^{-1} , revealed a short rubbery plateau with a typical modulus value: $E_R = 10 \text{ MPa}$ at 440 K, which corresponds to a critical molar weight $M_c \approx 1.3 \text{ kg mol}^{-1}$ against the literature value of 3 kg mol^{-1} .¹⁰

Tensile testing at ambient temperature, $7 \times 10^{-4} \text{ s}^{-1}$ deformation rate, revealed a ductile behavior, with a Young's modulus $E \approx 2.42 \text{ GPa}$, an upper yield stress $\sigma_y = 69 \text{ MPa}$, a lower yield stress $\sigma_{y1} \approx 53 \text{ MPa}$, and an ultimate stress $\sigma_\lambda = 75 \text{ MPa}$. The ultimate elongation was more than 100%.

Samples

The samples were machined from extruded plaques of 2 mm thickness. Dogbone samples having an active length of 50 mm, according to the French standard AFNOR NFT 51054, were used for mechanical testing. Squares of $100 \times 100 \text{ mm}$ were used for sorption (gravimetric) tests.

Exposure, Water Sorption

Exposure was made in previously described climatic chambers¹² allowing to study the 20–100°C temperature range and the 0–100% hygrometric ratio range. The water absorption was gravimetrically studied using a laboratory balance with a relative precision of 10^{-4} .

Hydrolysis Rate

The extent of chain scission was determined by SEC. The experimental details will be given in the next part of this article (Part II, this issue, page 174).

Physical Characterization

Differential scanning calorimetry was made using a SETARAM scanning calorimeter operating between 300 and 683 K, at 10 K min^{-1} scanning rate. The glass transition temperature T_g was taken at the inflexion point. Tensile testing was made on a ZWICK machine. In the range of small deformations ($\leq 10\%$), i.e., for modulus or yield measurements, a MTS extensometer was used. Larger deformations were determined from the crosshead displacement. This machine was equipped with an oven, allowing the determination of tensile characteristics in a large domain of temperatures and deformation rates.

RESULTS

Gravimetric Study of Water Absorption

The curves of water absorption at 40, 70, 80, and 90°C, 100% RH, are shown in Figure 1. The equilibrium water concentration M_m and the diffusion coefficient D are listed in Table I, and their variations with the temperature are presented in Figures 2 and 3. All these values are generally in agreement with the literature data.^{7,11,13}

The trends of variation of M_m with temperature can be resumed as follows:

$$\text{For } T \leq 343 \text{ K: } M_m \approx 0.3\%$$

$$\text{For } T > 343 \text{ K: } M_m = 0.3 + 8 \times 10^{-3} (T - 343)$$

In the domain under study, the equilibrium water content varies between 0.04 and 0.08 water moles per ester mole.

The coefficient of diffusion varies with the temperature according to

$$D = 6.13 \times 10^{-3} \exp\left(-\frac{3125}{T}\right) (\text{cm}^2 \text{ s}^{-1})$$

which corresponds to an apparent activation energy of 26 kJ mol^{-1} (30 kJ mol^{-1} by taking also in account the literature data).

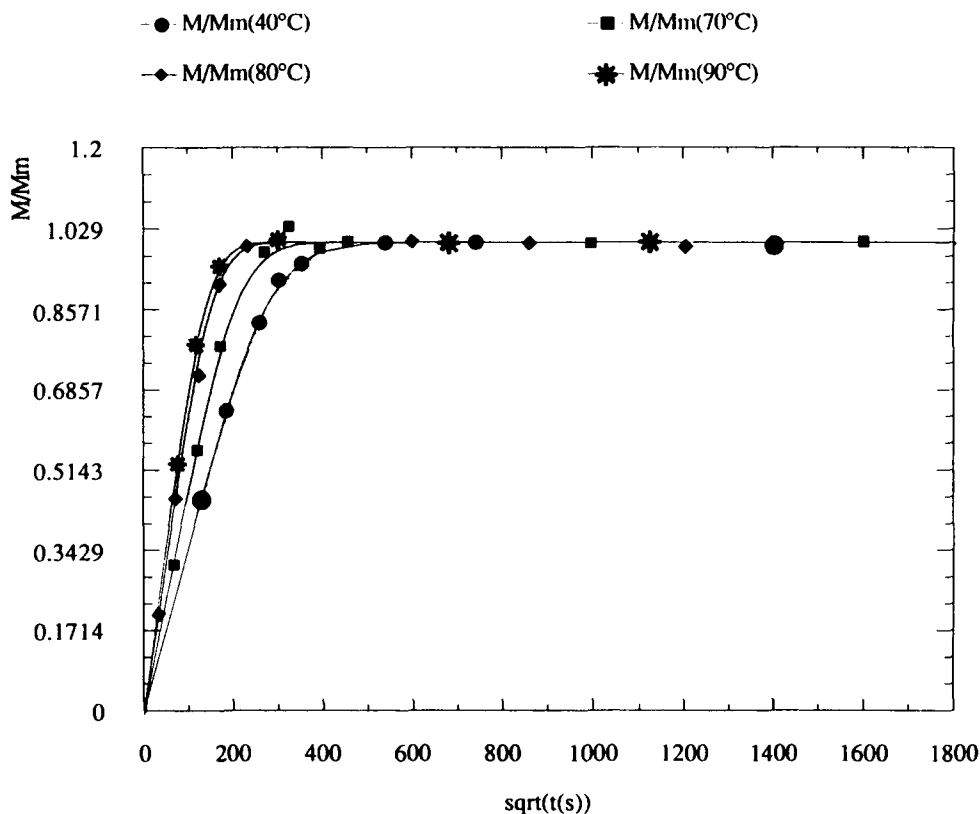


Figure 1 Gravimetric curves of water absorption. The temperatures are indicated on the figure.

Calorimetric Study

All the DSC measurements were made long after the sorption equilibrium was reached. In other words, the eventual changes are essentially due to irreversible aging rather than change of water concentration.

Typical thermograms (first scan) are shown in Figure 4(a). The most noticeable change concerns the apparition of two endotherms at, respectively, 430 K (just above T_g) and 470 K. These endotherms disappear in a second scan, Figure 4(a'). These features were already observed by Bair et al.¹⁶ and attributed to crystals of bisphenol A.

The thermograms of a bisphenol A sample from Fluka Chemika (purity: 97% from HPLC data) are presented in Figure 4(b). The first scan displays a melting point at 432 K. During the second scan, Figure 4(b'), a new exothermic peak (presumably crystallization peak) appears at 350 K whereas the melting endotherm is shifted to 409 K. All these characteristics were previously reported by Bair et al.¹⁶ They suggested the existence of two crystalline forms of bisphenol A. A third endotherm at 459 K is observed by these authors but it does not appear in our case.

The fusion enthalpy of bisphenol A, determined on the first run of Figure 4(b), is 57 J g^{-1} . The en-

Table I Equilibrium Water Concentration and Water Diffusivity Determined from Gravimetric Curves of Water Absorption

T ($^{\circ}\text{C}$)	M_m	D (cm^2/s)	$1/T$ ($1/\text{K}$)	$\ln(D)$
40	0.318277	2.95E-07	0.003195	-15.0363
70	0.295489	5.27E-07	0.002915	-14.4551
80	0.3649	9.75E-07	0.002833	-13.8406
90	0.4527	1.15E-06	0.002755	-13.6765

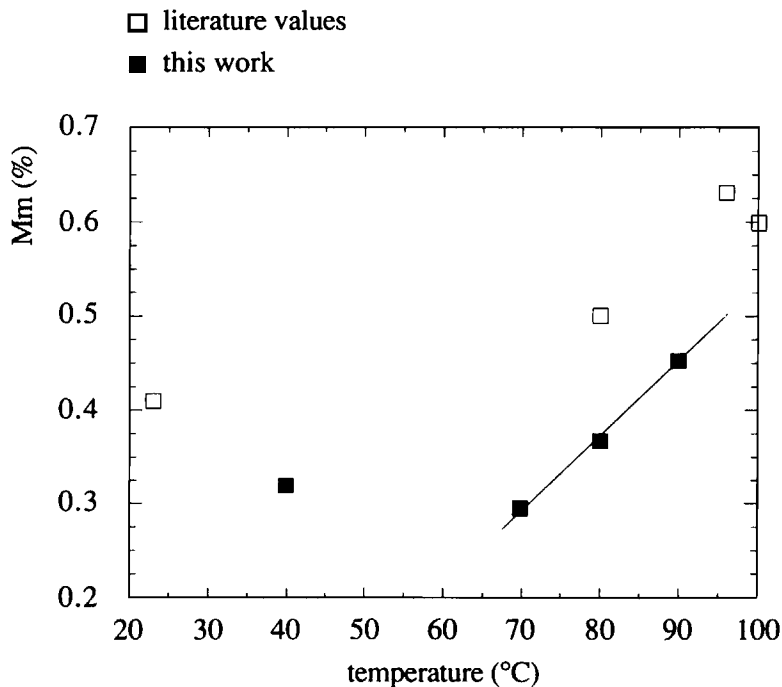


Figure 2 Influence of temperature on the equilibrium water concentration. Open symbols: literature values;^{18,19} closed symbols: this work.

thalpy of the endothermic process at 430 K determined on the first run of Figure 4(a) is 4.1 J g^{-1} , which would correspond to a weight fraction of bisphenol A in polycarbonate of about 7%. It is note-

worthy that the enthalpy relaxation associated with physical aging can contribute to the endotherm at 430 K,⁹ so that the above estimation of the bisphenol A weight fraction is probably largely overestimated.

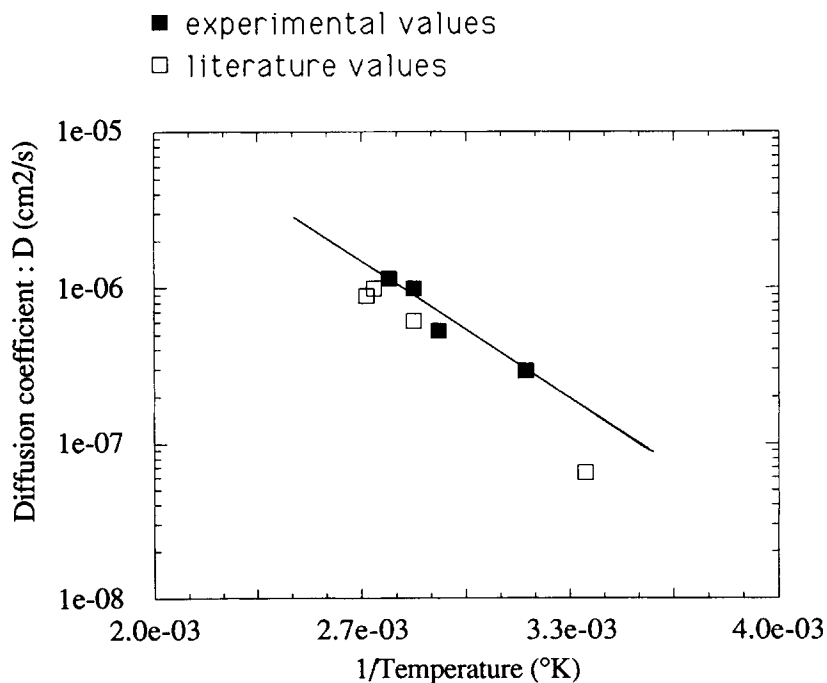


Figure 3 Arrhenius plot of the diffusion coefficient. Open symbols: literature values; closed symbols: this work.

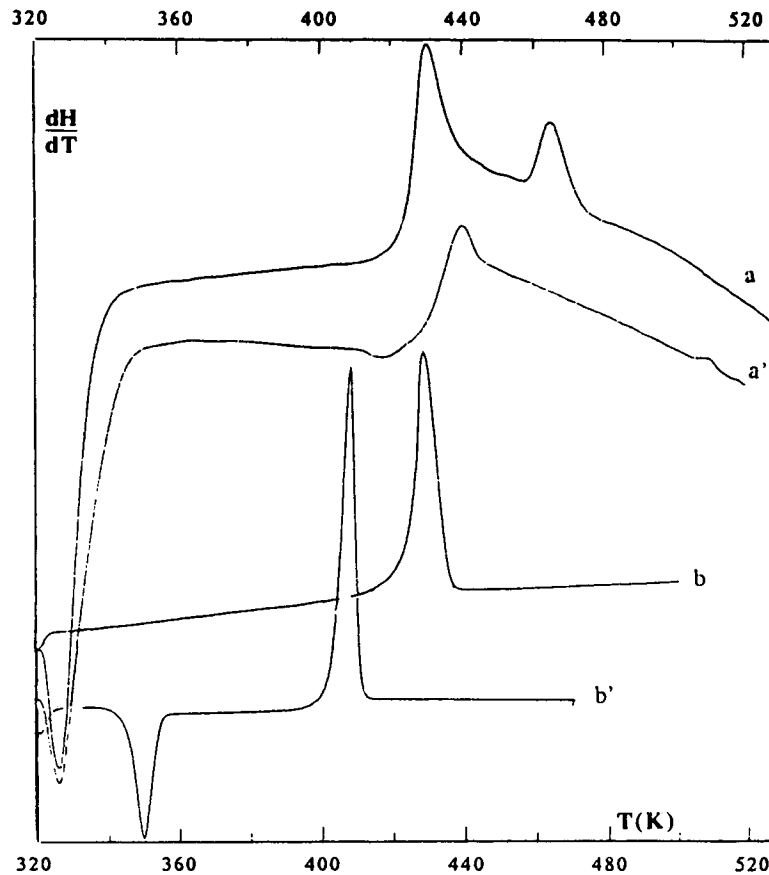


Figure 4 (a) DSC thermograms of a PC-aged sample. (b) DSC thermograms of BPA crystals.

The fact that this endotherm disappears during the second scan suggests that bisphenol A molecules are randomly redistributed into the polymer matrix upon melting and cannot recrystallize in the time scale of the experiment, owing to their presumably very low diffusivity in a such high-viscosity matrix.

Figure 5 displays T_g determined in the dry state at the inflexion point of the thermogram, against the reciprocal of number-average molar mass M_n determined by SEC. It can be seen that although T_g appears as a decreasing function of M_n^{-1} , the experimental points seem to be distributed into two distinct straightlines. The first one, which corresponds to the lower temperatures of exposure, i.e., 40 and 70°C, could be represented by:

$$T_g = 432 - \frac{265}{M_n} \quad (T_g \text{ in K, } M_n \text{ in kg mol}^{-1})$$

while the second line, which is nearly parallel to the first one, would be represented, for exposure temperatures of 80 and 90°C, by

$$T_g = 427 - \frac{219}{M_n}$$

Yield Properties

The upper yield stress σ_y , was determined before and after exposure, at various temperatures: 313, 328, 343, 353, and 363 K, and various deformation rates $\dot{\epsilon}$: 6.67, 66.7, 667, 1330, and 1667 $\times 10^{-4} \text{ s}^{-1}$.

An Eyring plot, $\sigma_y/T = f(\ln \dot{\epsilon})$, is presented in Figure 6 for the virgin sample. These results agree reasonably with the EYRING model:

$$\dot{\epsilon} = \dot{\epsilon}_0 \exp - \frac{Q - V\sigma}{RT}$$

The average slope of the straightlines is

$$\frac{R}{V} \approx 4 \times 10^3 \text{ Pa K}^{-1}$$

which corresponds to an activation volume of 2080 $\text{cm}^3 \text{ mol}^{-1}$, equivalent to about 10 monomer units (molar volume = 254/1.20 = 212 $\text{cm}^3 \text{ mol}^{-1}$).

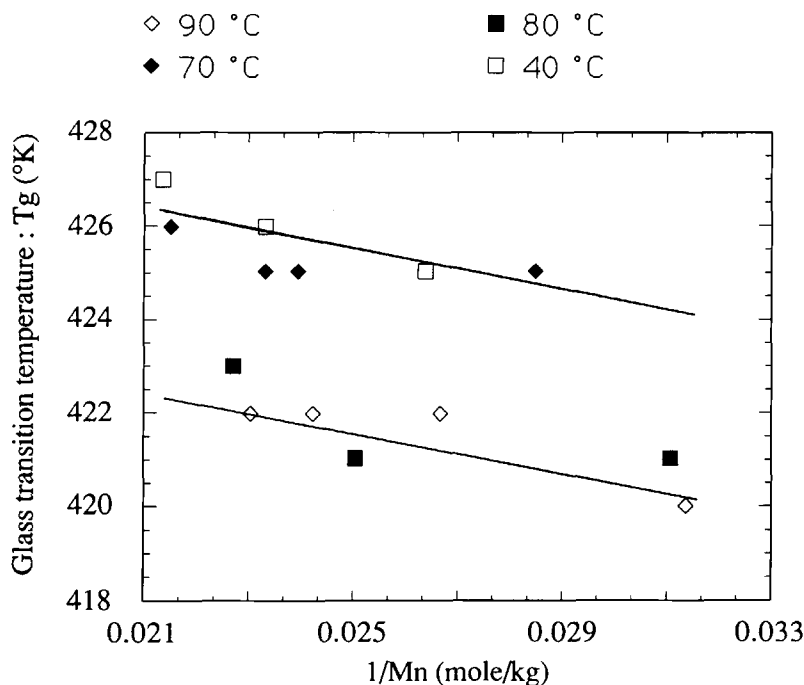


Figure 5 Glass transition temperature determined by DSC against reciprocal number-average molar mass determined by GPC. (□) 40°C, (◆) 70°C, (■) 80°C, (◇) 90°C.

The activation energy Q , determined from intercept values, would be $Q = 303 \text{ kJ mol}^{-1}$.

These values are in good agreement with the literature data.¹⁴ These same tests were performed for samples aged for 14 days at 60 and 80°C. The values reported are an average of two sets of measurements per temperature.

Table II summarizes the values obtained for the testing of samples aged for 14 days at 60 and 80°C, respectively.

It is evident that 14 days exposure at 60°C caused practically no degradation as found from SEC data. There is no significant change of Eyring parameters.

In contrast, exposure at 80°C causes a significant decrease (35%) of the activation volume. In other words, hydrolytic aging induces an increase of the rate sensitivity of the yield stress.

DISCUSSION

The observed water solubility (0.04 mol H₂O/mole monomer) at relatively low temperatures ($T < 340 \text{ K}$) is noticeably lower than the value predicted from simple molar additive rules ($M_m = 0.41 \text{ mol per mole of ester}$).⁴

It is interesting to note that it corresponds to only 7 mol water per chain, i.e., 3.5 mol water per

chain end. In other words, highly hydrophilic chain ends as, for instance, phenols, could play a significant role in water absorption.

A characteristic time of diffusion t_D can be determined from the experimental values of the diffusion coefficient D :

$$t_D = \frac{L^2}{D}$$

where L is the sample thickness (0.2 cm). Thus:

$$t_D = \frac{L^2}{D_0} \exp \frac{E_D}{RT} = 6.52 \exp \frac{3125}{T}$$

which leads to $t_D = 39 \text{ h}$ at 40°C and 10 h at 90°C.

Since most of the physical measurements have been made after exposure periods at least 10 times higher than t_D , it can be concluded that the results cannot be significantly influenced by water concentration changes due to diffusion. The problem of water consumption by the hydrolysis process will be examined in detail in the next part of this article (this issue), but it can be yet assumed that there are no depth degradation gradients in the samples under study.

The results of DSC measurements call for the following comments:

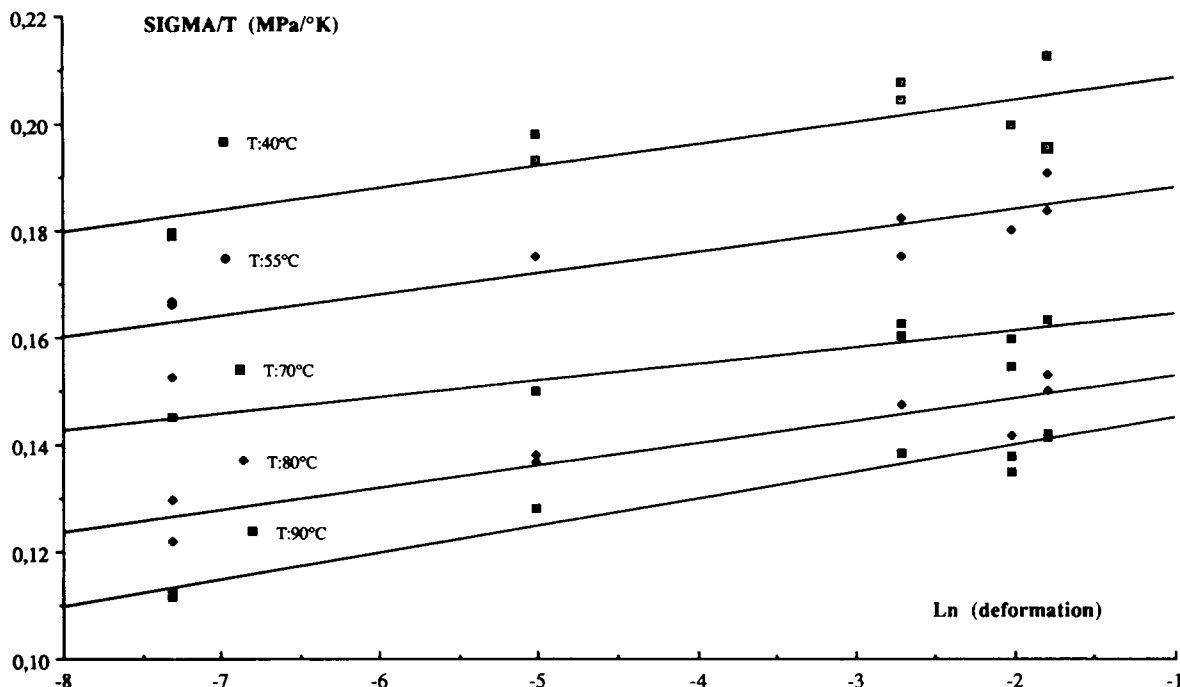


Figure 6 Eyring plot (reduced stress vs. logarithm of deformation rate) for the virgin sample.

1. Decrease of glass transition temperature: At low temperature (40 and 70°C), T_g decreases, when the molar mass decreases as a result of hydrolytic chain scission, according to the Fox-Flory law:¹⁵

$$T_g = T_{g\infty} - \frac{B}{M_n}$$

The values of $T_{g\infty}$ (432 K) and B (265 K kg mol⁻¹) could reasonably correspond to data relative to virgin polycarbonates differing by their molar mass.

Table II Slope of the Eyring Straight Line and Corresponding Activation Volume Against Aging Conditions

Samples	M_n	R/V	V (cm ³ /mol)
Virgin		4.3 ± 0.3	
Aged 40°C	46.5 ± 0.5	$\times 10^3 \text{ Pa K}^{-1}$	1930 ± 130
Aged 70°C		6.7 ± 0.1	
Aged 40°C	43.7 ± 0.3	$\times 10^3 \text{ Pa K}^{-1}$	1242 ± 19
Aged 70°C			

- At high temperature (80 and 90°C), there is a supplementary cause of T_g decrease in the early days of exposure. It seems logical to suppose that this decrease (≈ 5 K) is due to a physical rather than chemical (chain scission) mechanism. It could be, for instance, attributed to physical aging whose well-known consequence is to enhance the glass transition hysteresis responsible, at least partially, for the endotherm at 430 K. The apparent discontinuity observed between 70 and 80°C is consistent with the Bauwens's theory according to which distinct phenomena (annealing and physical aging) occur, respectively, above and below $T_g - \Delta T$ where $\Delta T \approx 50$ K.¹⁴ In the case of wet polycarbonate, it can be reasonably assumed that this limit is close to 70–80°C.
2. Endotherms at 430 and 470 K: These endotherms were attributed by Bair et al.¹⁶ to bisphenol (BPA) crystals. The following arguments are in favor of this interpretation:
 - a. Bair et al.¹⁶ reported calorimetric, microscopic, and chromatographic evidences of the presence of BPA crystals.
 - b. The endotherm at 430 K can be at least partially attributed to BPA melting.
 - c. The initially transparent samples become

more and more turbid as the exposure time increases. This is consistent with the hypothesis of crystal formation, although other possibilities (osmotic cracking) exist.

Concerning the nature of crystals, only three reasonable hypotheses can be made: (1) BPA crystals, (2) oligomer (e.g., dimer) crystals, and (3) polymer paracrystals. According to our results, the presence of BPA could explain the endotherm at 430 K. From the results of Figure 4(b), reservations are to be made on the attribution of the endotherm at 470 K to BPA. We lack data to choose between the oligomer and polymer paracrystal hypothesis for this latter peak. Oligomers were observed by Bair et al.¹⁶ in SEC chromatograms so that their presence would not be very surprising. Polymer paracrystals would have effectively a melting point lower than the polycarbonate one (608 K). When they are observed, for instance, in random copolymers such as ethylene-propylene rubbers (EPR), they display generally endotherms wider than the peak at 470 K observed here.

Some arguments against the hypothesis of BPA crystals can be also cited:

1. No BPA peak was observed in SEC chromatograms.
2. To explain ultraviolet spectrophotometric observations, Pryde et al.² suggested that hydrolysis would occur preferentially at chain ends.

This behavior involves necessarily an interaction between the terminal OH group and the last carbonate group. Such interaction can only result from backbiting—but it is prevented here by the relatively high chain stiffness—or from inductive/mesomeric effects—but they are in principle prevented by the rupture of the conjugation by the isopropylidene group. So, it seems difficult to justify, theoretically, this hypothesis of crystal formation.

3. From SEC data, it can be estimated that for the sample of Figure 4(a), the number of chain scissions per mass unit is less than $20 \times 10^{-3} \text{ mol kg}^{-1}$, which corresponds to a conversion ratio less than 5×10^{-3} (Part II, this issue).

For such low conversion, a simple statistical approach shows that the BPA yield must be about 2% of the total chain scission yield for a polymer of $DP_n = 100$. In this case, the mass fraction of BPA re-

sulting from random chain scission would be less than 0.01%, i.e., insignificant relative to the initial BPA content (1 to 2% according to Bair et al.¹⁶), and obviously unable to induce the phase separation needed for BPA crystallization.

It is our understanding that the only way to conciliate these apparently contradictory data is the hypothesis of heterogeneous degradation. Hydrolysis would be very fast in localized microdomains where it could lead to relatively high BPA yields. This localization is, indeed, favorable to further BPA crystallization.

An expected consequence of such heterogeneity is a strong increase of the polydispersity, which was not observed experimentally. The hypothesis remains, however, valid if the volume fraction of microdomains is very low in such a way as low molecular weight hydrolysis products are practically undetectable by SEC. Does the heterogeneity preexist or is it induced by hydrolytic aging? We lack data to answer this question; supplementary investigations are needed to elucidate these mechanisms.

The aging-induced changes of tensile yield behavior call for the following comments: It is well known that yield stress is sensitive to physical aging,⁹ but this latter can be represented by a translation of $(\sigma_y/T - \dot{\epsilon})$ straight lines in the Eyring's plot.¹⁷ Here, there is also a slope change since the activation volume decreases from 2000 to 1200 cm³ mol⁻¹. It appears thus that other processes than physical aging, presumably hydrolytic degradation, play a significant role in the change of yield behavior.

Here, also, highly degraded microdomains could act as defects responsible for stress concentration leading to the observed change of kinetic regime.

CONCLUSIONS

The polycarbonate hydrolysis displays two apparently contradictory features: according to SEC data, it is too low to be diffusion controlled so that chain scissions are expected to be homogeneously distributed into the sample thickness.

According to DSC data, it is probably heterogeneous since hydrolytic aging leads to the formation of bisphenol A and presumably oligomer crystals, a phenomenon that disagrees with the hypothesis of random chain scission.

These results lead us to postulate the existence of a dual mechanism:

1. Homogeneous, low-rate, random chain scission responsible for the molar weight decrease observed by SEC.

2. High-rate chain scission localized in microdomains of very low volume fraction and responsible for BPA formation.

The change of physical properties can therefore result from at least three distinct phenomena:

1. Random chain scission, responsible for T_g decrease according to Fox and Flory, with $dT_g/d(M_n^{-1}) \approx -250 \text{ K kg mol}^{-1}$.
2. Physical aging (annealing effects) responsible for a T_g decrease of about 5 K in the early days of exposure and presumably for an increase of the yield stress.
3. Formation of morphological defects (crystals of low-molecular-weight degradation products), responsible for the sample turbidity and that could play a role in the change of the rate sensitivity of the yield stress.

The authors wish to express their gratitude for the generous support received from Dr. D. Valentin in the beginning of this research. Thanks are also expressed to J. C. Teissedre, Centre des Matériaux de l'E.M.P., for his help in conducting mechanical experiments.

REFERENCES

1. G. D. Cooper and B. J. Williams, *Organ. Chem.*, **27**, 3717 (1962).
2. C. A. Pryde and M. Y. Hellman, *J. Appl. Polym. Sci.*, **25**, 2573 (1980).
3. F. C. Schilling, W. M. Ringo, N. J. A. Sloane, and F. A. Bovey, *Macromolecules*, **14**, 532 (1981).
4. H. E. Bair, D. R. Falcone, M. Y. Hellman, G. E. Johnson, and P. G. Kelleher, *J. Appl. Polym. Sci.*, **26**, 1777 (1980).
5. C. A. Pryde, P. G. Kelleher, M. Y. Hellman, and R. P. Wentz, *Polym. Eng. Sci.*, **22**, 370 (1982).
6. P. G. Kelleher, R. P. Wentz, M. Y. Hellman, and E. H. Gilbert, *Polym. Eng. Sci.*, **23**, 10 (1983).
7. A. Golovoy and M. Zimbo, *Polym. Eng. Sci.*, **29**, 29 (1984).
8. R. J. Gardner and J. R. Martin, *Spe ANTEC Tech. Papers*, **24**, 328 (1978).
9. L. C. E. Struik, *Physical Ageing of Amorphous Polymers and Related Materials*, Elsevier, Amsterdam, 1978.
10. D. W. Van Krevelen and P. J. Hoffer, *Properties of Polymers and Their Correlation with Structure*, 2nd ed., Elsevier Amsterdam, 1976, p. 339.
11. L. M. Robeson and S. T. Crisafulli, *J. Appl. Polym. Sci.*, **28**, 2925 (1983).
12. P. Bonniau, *Effets de l'absorption d'eau sur les propriétés électriques et mécaniques des matériaux composites à matrice organique*, Thèse Ecole Nationale Supérieure des Mines de Paris, March 21 (1983).
13. M. Narkis, S. Sibony, L. Nicolais, A. Paicella, and R. J. Gardner, *Polym. Comm.*, **26**, 339 (1985).
14. J. C. Bauwens and C. Bauwens-Crowet, *J. Mater. Sci.*, **14**, 1817 (1979).
15. T. G. Fox and P. J. Flory, *J. Appl. Phys.*, **21**, 551 (1950).
16. H. E. Bair, D. R. Falcone, M. Y. Hellman, G. E. Johnson, and P. G. Kelleher, *J. Appl. Polym. Sci.*, **26**, 1777 (1981).
17. S. Matsuoka, in W. Brostow and R. D. Corneliussen, Eds., *Failure of Plastics*, SPE/Hanser, Munich, 1986, Chap. 3, pp. 50-52.
18. T. L. Smith, *J. Polym. Sci.*, **20**, 447, (1956).
19. G. Menges, in *Failure of Plastics*, W. Brostow and R. D. Corneliussen, Eds., SPE/Hanser, New York, 1986, Chap. 13, p. 259-272.

Received March 10, 1993

Accepted September 27, 1993